REPORT DOCUMENTATION PAGE

Form Approved
OMB NO. 0704-0188

1. AGENCY USE ONLY (Leave Blank)

2. REPORT DATE 08/23/05

3. REPORT TYPE AND DATES COVERED
Final: June 1, 2002 - May 31, 2005

4. TITLE AND SUBTITLE
Quantum Computing Graduate Research Program: Gradiometer INSQUID

5. FUNDING NUMBERS
DAAD 19-02-1-0187

6. AUTHOR(S)
John Clarke

7. PERFORMING ORGANIZATION NAME(S) AND ADDRESS(ES)
University of California, Berkeley
336 Sproul Hall #5940
Berkeley, CA 94720-5940

8. PERFORMING ORGANIZATION REPORT NUMBER
ARO/JC/05

9. SPONSORING / MONITORING AGENCY NAME(S) AND ADDRESS(ES)
U. S. Army Research Office
P.O. Box 12211
Research Triangle Park, NC 27709-2211

10. SPONSORING / MONITORING AGENCY REPORT NUMBER
44059.9-PH-QC

11. SUPPLEMENTARY NOTES
The views, opinions and/or findings contained in this report are those of the author(s) and should not be construed as an official Department of the Army position, policy or decision, unless so designated by other documentation.

12 a. DISTRIBUTION / AVAILABILITY STATEMENT
Approved for public release; distribution unlimited.

12 b. DISTRIBUTION CODE

13. ABSTRACT (Maximum 200 words)

This project is focused on developing flux qubits, understanding sources of relaxation and decoherence, and investigating entanglement of two qubits. This report describes our progress toward these goals over the last three years. We outline the infrastructure of our experiment and chip fabrication process, and describe a novel, dual-current source source to supply two independent flux biases to the qubits and readout SQUID. We present results showing quantum coherence in a flux qubit, including spectroscopy, Rabi oscillations, Ramsey fringes, spectroscopic linewidths, and spin echoes. The different kinds of decoherence times deduced from the last three experiments are shown to be self-consistent. We summarize a study of the effects of nonequilibrium quasiparticles generated in the readout SQUID when it switches to the voltage state. These excess quasiparticles are shown to persist for a remarkably long time, about 1 ms, and thus set an upper limit on the repetition rate at which data can be acquired. We describe the theory of a novel device for entangling two flux qubits by means of a single SQUID that serves also as the readout device. It is shown that this scheme is in principle capable of the CNOT (Controlled NOT) operation.

14. SUBJECT TERMS
Quantum computing, flux qubits, variable inductance coupling, entanglement of qubits, single-shot readout, relaxation and decoherence of qubits, back-action, hot quasiparticles.

15. NUMBER OF PAGES
18

16. PRICE CODE

17. SECURITY CLASSIFICATION OR REPORT	18. SECURITY CLASSIFICATION ON THIS PAGE	19. SECURITY CLASSIFICATION OF ABSTRACT	20. LIMITATION OF ABSTRACT
UNCLASSIFIED	UNCLASSIFIED	UNCLASSIFIED	UU

NSN 7540-01-280-5500

Standard Form 298 (Rev.2-89)
Prescribed by ANSI Std. 239-18
298-102

REPORT DOCUMENTATION PAGE (SF298)
(Continuation Sheet)

Papers and Presentations

(a) Manuscripts submitted: None.
(b) Papers published:

1. Flux Qubit Completes the Hat Trick, John Clarke, *Science* **299**, 1850 (2003).

2. Vortices and Hearts, John Clarke, *Nature* News and Views, **425,** 133 (2003).

3. Low-Noise Computer-Controlled Current Source for Quantum Coherence Experiments, S. Linzen, T.L. Robertson, T. Hime, B.L.T. Plourde, P.A. Reichardt, and John Clarke, *Rev. Sci. Instrum.* **75**, 2541 (2004).

4. Decoherence in Josephson-junction Qubits due to Critical Current Fluctuations, D.J. Van Harlingen, T.L. Robertson, B.L. T. Plourde, P.A. Reichardt, T.A. Crane, and John Clarke, *Phys. Rev. B*, **70**, 064517 (2004).

5. Entangling Flux Qubits with a Bipolar Dynamic Inductance, B.L.T. Plourde, J. Zhang, K.B. Whaley, F.K. Wilhelm, T.L. Robertson, T. Hime, S. Linzen, P.A. Reichardt, C.-E. Wu and John Clarke, *Phys. Rev. B*, **70**, 140501 (2004).

6. Measurements of l/f Noise in Josephson Junctions at Zero Voltage: Implications for Decoherence in Superconducting Quantum Bits," Michael Mück, Matthias Korn, C.G.A. Mugford, J.B. Kycia and John Clarke, *Appl. Phys. Lett.*, **86**, 012510 (2005).

7. Superconducting Quantum Interference Device with Frequency-Dependent Damping: Readout of Flux Qubits, T.L. Robertson, B.L.T. Plourde, T. Hime, S. Linzen, P.A. Reichardt, F.K. Wilhelm and John Clarke, *Phys. Rev. B*, **72**, 024513-023521 (2005).

8. Flux Qubits and Readout Device with Two Independent Flux Lines, B.L.T. Plourde, T.L. Robertson, P.A. Reichardt, T. Hime, S. Linzen, C.-E. Wu and John Clarke, *Phys. Rev. B*, **72**, 060506 (2005).

(c) Papers published in conference proceedings: None
(d) Papers presented at meetings:

1. "Critical Current 1/f Noise in Josephson Junctions: Implications for Flux Qubits," John Clarke, AFOSR Review, Cambridge, MA, July, 2002

2. "RC-shunted SQUIDs for Single-shot Measurement of Flux Qubits," invited talk, B.L.T. Plourde, T.L. Robertson, P.A. Reichardt, T. Hime, D.J. Van Harlingen, J. Clarke, Applied Superconductivity Conference, Houston, TX, August 9, 2002.

3. "Characterization and implications of low frequency noise in superconducting phase qubits," invited talk, D.J. Van Harlingen, B.L.T. Plourde, T.L. Robertson, P.A. Reichardt, R. Therrien, J. Clarke, LT 23, Hiroshima, Japan, August, 2002.

4. "Decoherence in Flux Qubits due to l/f Noise," T.L. Robertson, D.J. Van Harlingen, B.L.T. Plourde, P.A. Reichardt and J. Clarke, March Meeting of the American Physical Society, Austin, Texas, March 3-7, 2003.

5. "RC-Shunted SQUIDs for Single-Shot Measurement of Flux Qubits," B.L.T. Plourde, T.L. Robertson, T. Hime, S. Linzen, P.A. Reichardt, J. Clarke and D.J. Van Harlingen, March Meeting of the American Physical Society, Austin, Texas, March 3-7, 2003.

6. "Critical Current l/f Noise in Josephson Junctions: Implications for Flux Qubits," Tim Robertson, Britton Plourde, Paul Reichardt, Dale Van Harlingen and John Clarke, invited talk by John Clarke at Wilhelm und Else Heraeus-Stiftung Seminar, "Challenges of Applied Cryoelectrics II" Weilburg, Germany, May 26-28, 2003.

7. "l/f Noise in the Critical Current of Josephson Junctions: Implications for Flux Qubits," John Clarke, seminar, Department of Microtechnology and Nanoscience, Chalmers University of Technology, Gothenburg, Sweden, June 16, 2003.

8. "Progress in Flux Qubits," John Clarke, seminar, Department of Microtechnology and Nanoscience, Chalmers University of Technology, Gothenburg, Sweden, June 16, 2003.

9. "Use of RC-Shunted SQUIDs for Single-Shot Readout of Flux Qubits," T.L. Robertson, B.L.T. Plourde, S. Linzen, P.A. Reichardt, T. Hime, and J. Clarke, 9th International Superconductive Electronics Conference (ISEC 2003), Sydney, Australia, July 7-11, 2003.

10. "Decoherence in Superconducting Qubits from l/f Noise," D.J. Van Harlingen, T.A. Crane, B.L.T. Plourde, T.L. Robertson P.A. Reichardt and John Clarke, invited talk by Dale Van Harlingen, Sixth European Conference on Applied Superconductivity (EUCAS), Sorrento, Italy, September 14-18, 2003.

11. "Backaction in SQUID-Readout of a Flux Qubit," John Clarke, invited talk at the International Conference on Solid State Quantum Information Processing, Amsterdam, The Netherlands, December 19, 2003

12. "Macroscopic Quantum Coherence In Superconducting Devices: Flux Qubits," Britton Plourde, Syracuse University, Physics Colloquium, February 3, 2004.

13. "The Ubiquitous Flux Vortex: SQUIDs, Qubits and Dynamics," Britton Plourde, Syracuse University, Condensed Matter Seminar, February 4, 2004.

14. "Quantum Coherence in Nanoscale Superconducting Devices: Flux Qubits," Britton Plourde, University of Massachusetts, Condensed Matter Seminar, February 17, 2004.

15. "Quantum Coherence In Nanoscale Superconducting Devices: Flux Qubits," Britton Plourde, University of Minnesota, Condensed Matter Seminar, February 19, 2004.

16. "Flux Qubits: Readout, Hot Electrons and Adjustable Coupling," John Clarke, invited talk, International Symposium on Mesoscopic Superconductivity and Spintronics, Atsugi, Japan, March 4, 2004.

17. "Spectroscopy of Large Inductance Flux Qubits," T.L. Robertson, T. Hime, S. Linzen, B.L.T. Plourde, P.A. Reichardt, C.E. Wu, F.K. Wilhelm and John Clarke, March Meeting of the American Physical Society, Montréal, Canada, March 22-26, 2004.

18. "Back-Action of RC-Shunted SQUID on Three-Junction Flux Qubit," T. Hime, S. Linzen, B.L.T. Plourde, P.A. Reichardt, T.L. Robertson, C.E. Wu, F.K. Wilhelm and John Clarke, March Meeting of the American Physical Society, Montréal, Canada, March 22-26, 2004.

19. "Variable Coupling Scheme for Entangling Flux Qubits," B.L.T. Plourde, J. Zhang, T.L. Robertson, T. Hime, S. Linzen, P.A. Reichardt, C.E. Wu, K.B. Whaley, F.K. Wilhelm and John Clarke, March Meeting of the American Physical Society, Montréal, Canada, March 22-26, 2004.

20. "Decoherence of Flux Qubits Due to Hot Quasiparticles in Readout SQUID," P.A. Reichardt, T. Hime, S. Linzen, B.L.T. Plourde, T.L. Robertson, C.E. Wu, F.K. Wilhelm and John Clarke, March Meeting of the American Physical Society, Montréal, Canada, March 22-26, 2004.

21. "Dephasing from l/f Critical Current Fluctuations in Superconducting Qubits," T.A. Crane, D.J. Van Harlingen, T.L. Robertson, B.L.T. Plourde, P.A. Reichardt and John Clarke, March Meeting of the American Physical Society, Montréal, Canada, March 22-26, 2004.

22. "Measurements of the l/f Noise in Josephson Junctions for Potential Use as Qubits," Chas Mugford, Jan Kycia, Matthias Korn, Michael Mueck and John Clarke, March Meeting of the American Physical Society, Montréal, Canada, March 22-26, 2004.

23. "Flux Qubits: Controllable Coupling, Adjustable Relaxation Rate and l/f Noise," John Clarke, plenary invited talk, IV International Conference on Macroscopic Quantum Coherence and Computing, Napoli, Italy, June 7-10, 2004.

24. Conference Summary, John Clarke, invited closing address, IV International Conference on Macroscopic Quantum Coherence and Computing, Napoli, Italy, June 7-10, 2004.

25. "Large Inductance Flux Qubits: Coherent Manipulation and Controllable Coupling," John Clarke, Quantum Computing Program Review, Orlando, Florida, August 16-20, 2004.

26. "Back-Action of RC-Shunted SQUID on Three-Junction Flux Qubit," T. Hime, S. Linzen, B.L.T. Plourde, P.A. Reichardt, T.L. Robertson, C.-E. Wu, F.K. Wilhelm and John Clarke, Quantum Computing Program Review, Orlando, Florida, August 16-20, 2004.

27. "Superconducting flux qubits: readout, dynamics, and coupling," Britton L.T. Plourde, John Clarke, Travis Hime, Sven Linzen, Paul Reichardt, Tim Robertson, Birgitta Whaley, Frank Wilhelm, Cheng-En Wu, Jun Zhang, International Workshop on Solid State Based Quantum Information Processing, Herrsching, Bavaria, September 13-17, 2004.

28. "Superconducting flux qubits: readout, dynamics, and coupling," Britton L.T. Plourde, John Clarke, Travis Hime, Sven Linzen, Paul Reichardt, Tim Robertson, Birgitta Whaley, Frank Wilhelm, Cheng-En Wu, Jun Zhang, Quantum Information Science Seminar, Department of Physics, University of Illinois at Urbana-Champaign, September 29, 2004.

28. "Measurements of the 1/f Noise in Josephson Junctions for Potential Use as Qubits," Chas Mugford, Jan Kycia, Matthias Korn, Michael Mück and John Clarke, October 6, 2004, "Harnessing the Magic," Applied Superconductivity Conference, Jacksonville, Florida, October 3-8, 2004.

30. "Superconducting Flux Qubits: Coherent Oscillations, Controllable Coupling and 1/f Noise," John Clarke, seminar, University of Karlsruhe, Karlsruhe, Germany, November 10, 2004.

31. "Superconducting Flux Qubits: Coherent Oscillations and Controllable Coupling," John Clarke, seminar, Department of Physics, University of Copenhagen, Denmark, November 16, 2004.

32. "Superconducting Flux Qubits: Coherent Oscillations, Controllable Coupling and 1/f Noise," John Clarke, seminar, NEC Tsukuba, Japan, November 19, 2004.

33. "Large Inductance Flux Qubits: Coherent Manipulation and Controllable Coupling," John Clarke, invited talk, Wilhelm and Else Heraeus-Seminar, *Processing of Quantum Information in RSFQ Circuits and Qubits*, Bad Honnef, Germany, November 29, 2004.

34. "Flux Qubits and Readout Device with Two Independent Flux Lines," B.L.T. Plourde, T.L. Robertson, T. Hime, P.A. Reichardt, C.-E. Wu and John Clarke, March Meeting of the American Physical Society, Los Angeles, California, March 21-25, 2005.

35. "Quantum Coherence in a Superconducting Flux Qubit," T. Hime, B.L.T. Plourde, P.A. Reichardt, T.L. Robertson, C.-E. Wu and John Clarke, March Meeting of the American Physical Society, Los Angeles, California, March 21-25, 2005.

36. "Measurements of Dephasing in Superconducting Flux Qubits," C.-E. Wu, T. Hime, B.L.T. Plourde, P.A. Reichardt, T.L. Robertson and John Clarke, March Meeting of the American Physical Society, Los Angeles, California, March 21-25, 2005.

37. "Measurements of Relaxation in Superconducting Flux Qubits," P.A. Reichard, T. Hime, B.L.T. Plourde, T.L. Robertson, C.-E. Wu and John Clarke, March Meeting of the American Physical Society, Los Angeles, California, March 21-25, 2005.

38. "Flux Qubits and Readout Device with Two Independent Flux Lines," B.L.T. Plourde, T.L. Robertson, T. Hime, S. Linzen, P.A. Reichardt, C.-E. Wu, John Clarke, K. Birgitta Whaley, J. Zhang, and Frank Wilhelm, "Solid State and Optics" seminar, Yale University, "April 6, 2005.

39. "Large-Inductance Superconducting Flux Qubits: Coherent Oscillations and Controllable Coupling", John Clarke, seminar, M.I.T., Cambridge, Massachusetts, April 11, 2005.

40. "Large-Inductance Superconducting Flux Qubits: Coherent Oscillations and Controllable Coupling," John Clarke, seminar, Physics Department, Michigan State University, East Lansing, Michigan, April 25, 2005.

41. "Large-Inductance Superconducting Flux Qubits: Coherent Oscillations and Controllable Coupling," John Clarke, seminar, Interdisciplinary Research Center for Superconductivity, University of Cambridge, England, May 3, 2005.

42. "Flux Qubits and Readout Device with Two Independent Flux Lines," B.L.T. Plourde, T.L. Robertson, T. Hime, S. Linzen, P.A. Reichardt, C.-E. Wu, John Clarke, K. Birgitta Whaley, J.Zhang, and Frank Wilhelm, seminar, Institute for Quantum Computing, University of Waterloo, IQC Seminar, May 9, 2005.

43. "Superconducting Flux Qubits; Quantum Coherence in a Macroscopic Circuit," John Clarke, invited talk, Science Day 2005, Lawrence Livermore National Laboratory, May 23, 2005.

Table of Contents

List of Illustrations (Figures)

Technical Reports Submitted to ARO

1. Interim report dated 5/15/03 for period 6/1/02 to 12/31/02
2. Interim report dated 3/18/04 for period 1/1/03 to 12/31/03
3. Interim report dated 9/30/04 for period 1/1/04 to 7/31/04.

List of participating scientific personnel

Travis Hime, Graduate Student. No advanced degrees earned while employed on the project.

I. Introduction

This project is concerned with the fabrication and investigation of superconducting flux qubits, particularly with regard to the effects of dissipation on their relaxation and decoherence, and to the entanglement of two qubits. This final report summarizes the progress that we have made towards achieving these goals over the last three years. Section II outlines the infrastructure of our experiment, including the dilution refrigerator, the electrical filtering of the various leads associated with the measurements, a novel, dual-current source to supply two independent flux biases to the qubits and readout SQUID, the chip layout, and the fabrication process. Section III describes our results on achieving quantum coherence in a flux qubit, including spectroscopy, Rabi oscillations, Ramsey fringes, spectroscopic linewidths, and spin echoes. The different kinds of decoherence times deduced from the last three experiments are shown to be self-consistent. Section IV describes a study of the effects of nonequilibrium quasiparticles generated in the readout SQUID when it switches to the voltage state. These excess quasiparticles are shown to persist for a remarkably long time, about 1 ms, and thus set an upper limit on the repetition rate at which data can be acquired. Section V describes the theory of a novel device for entangling two flux qubits by means of a single SQUID that serves also as the readout device. It is shown that this scheme is in principle capable of the CNOT (Controlled NOT) operation. Section VI contains our concluding remarks.

II. Experimental Configuration

In order to observe quantum coherence in a superconducting circuit, it is necessary not only to cool it to low temperatures—say, a few tens of millikelvin—but also to isolate it from thermal and environmental noise generated at room temperature and at lower temperatures within the refrigerator itself. Thus, one needs to design a series of filters and attenuators that provide large levels of attenuation at room temperature, 4.2 K and certain temperatures between 4.2 K and the temperature of the experiment. Furthermore, it is of great importance that the qubit and its readout SQUID (Superconducting Quantum Interference Device) are coupled to impedances that are high enough to ensure that any Johnson noise currents injected into the quantum circuit are unimportant yet devoid of parasitic resonances at frequencies relevant to the operation of the qubit, typically a few gigahertz.

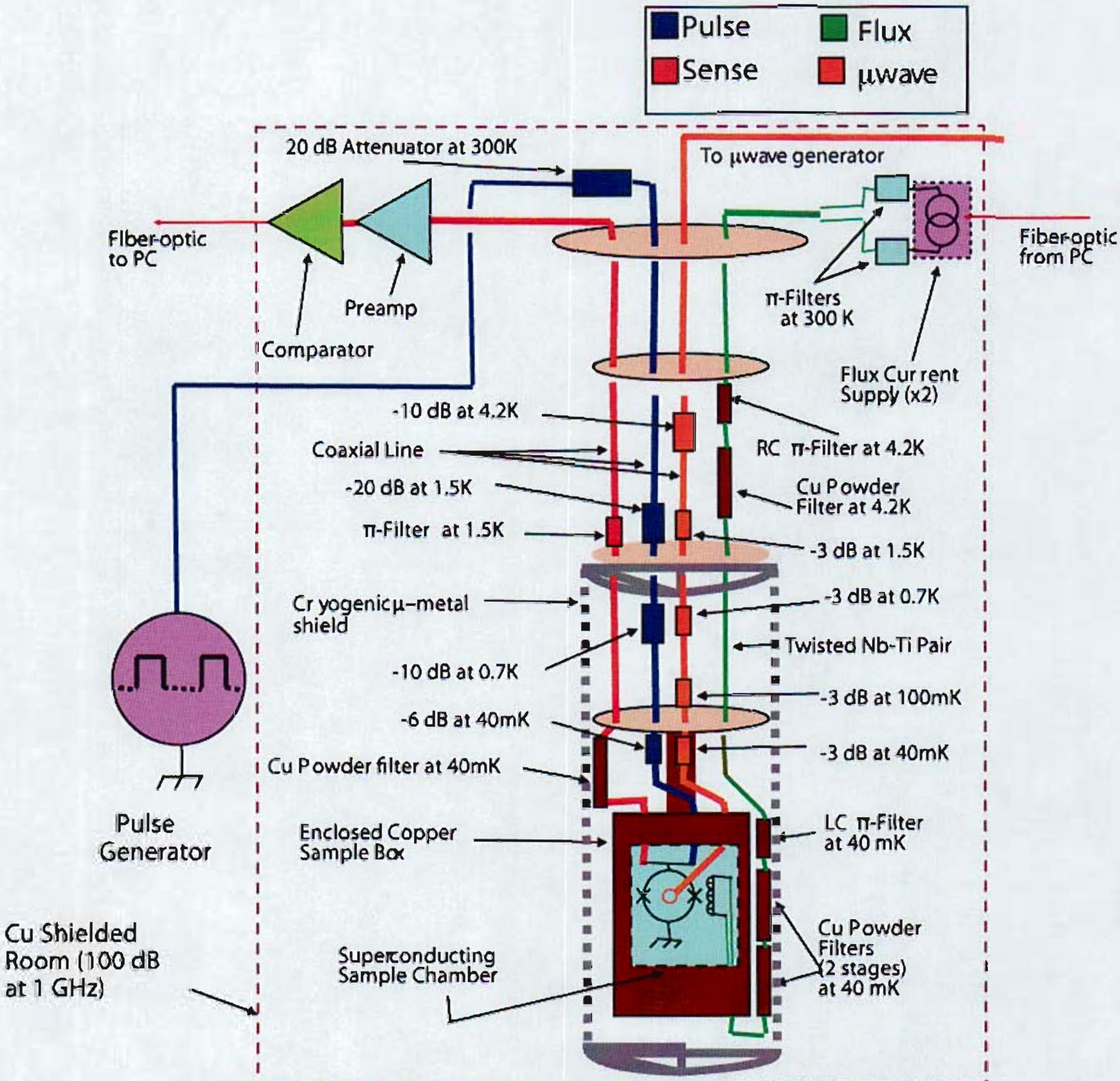

Fig. 1 Experimental configuration.

Figure 1 shows schematically the configuration of the measurement system. The dilution refrigerator is surrounded by a solid copper shielded room with an attenuation of 100 dB at 1 GHz. The refrigerator, an Oxford Kelvinox 300, is capable of attaining temperatures below 20 mK; however, the thermal load of the various wires and cables limits the base temperature to 35–40 mK. The chip on which the superconducting circuits are fabricated is mounted in the copper box. The cavity surrounding the chip is coated with lead and closed with a lead-coated lid (not shown) so that the circuits are enclosed in a superconducting cavity. The copper box is thermally anchored to the mixing chamber. The pulse and sense lines for the readout SQUID enter from the right-hand cavity, and are heavily damped by 3 kΩ resistors. The two flux bias lines, one for the qubit and the other for the readout SQUID, enter from the left and are heavily damped by copper powder filters [1] in the cavity (not shown). Finally, microwaves can be coupled to the qubit via a coaxial line that enters from below and is coupled to the qubit via a 1-mm-diameter loop of niobium wire.

Figure 1 shows the various levels of filters and attenuators. To determine the critical current of the readout SQUID, a current pulse is supplied by a computer-controlled generator outside the shielded room.

This line has a 20-dB attenuator at room temperature, a 20-dB attenuator at 1.5 K, a 10-dB attenuator at 0.7 K and a 6-dB attenuator at 40 mK. The pulse is largely reflected by the 3-kΩ terminating resistor, but the reflected pulse is absorbed by the matched 50-Ω attenuator at 40 mK so that there is no resonance. The sense line is coupled to the readout SQUID via a 3-kΩ resistor, and the signal passes through a copper powder filter at 40 mK and a π-filter at 1.5 K before being coupled to the room-temperature, battery-operated preamplifier. If the SQUID switches in response to the pulse, the comparator transmits a signal to the computer outside the shielded room via a fiber-optic link. The flux bias currents are very heavily filtered: there are π-filters at 300 K and 4.2 K, a copper powder filter at 4.2 K, and a π-filter and two copper powder filters at 40 mK. This series of filters roll off sharply at frequencies above 25 Hz. Finally, the microwave generator, which is outside the shielded room, is inductively coupled to the qubit via a line with the following attenuators: 20 dB at room temperature, 10 dB at 4.2 K, 3 dB at 1.5 K, 3 dB at 100 mK and 3 dB at 40 mK. In addition, there is a high pass filter at 10 MHz. The mutual inductance of the line to the qubit is extremely small, approximately 10 fH.

The low-temperature stage of the refrigerator is surrounded by a cryogenic mu-metal shield that reduces the earth's magnetic field to below 1 μT.

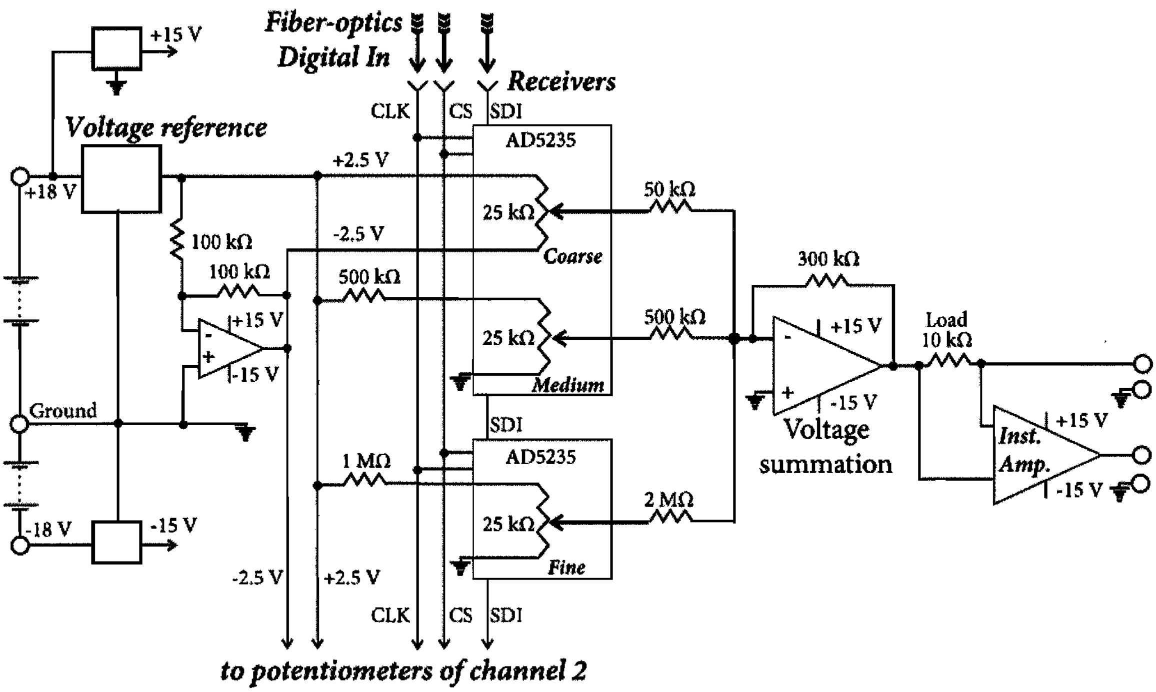

Fig. 2 Schematic of current source.

Flux bias currents are produced by digitally programmable potentiometers controlled by computer over a fiber-optic link [2]. This circuit, shown schematically in Fig. 2, consists of two current channels each with a maximum output of ±1 mA and an accuracy of about ±1 nA. The current source was designed not to inject digital noise into the qubit, and measured noise currents are sufficiently low to contribute negligibly to observed decoherence. The low noise of the current source combined with the shielding from the superconducting cavity provides high flux stability in the system, allowing for experimental runs of up to 48 hours.

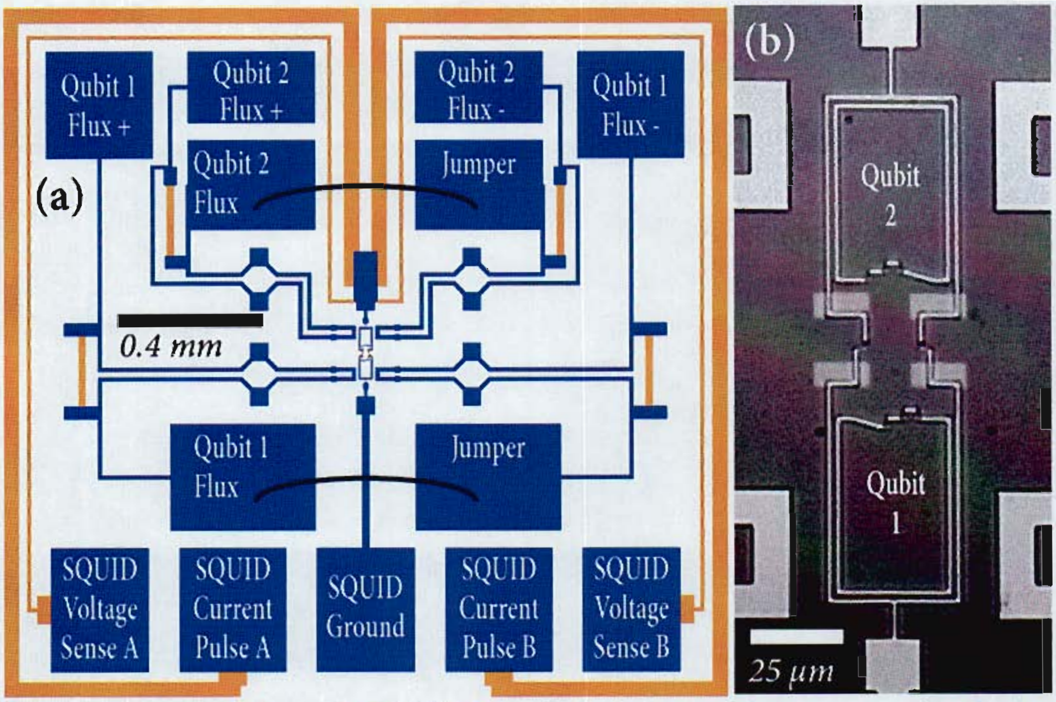

Fig. 3 Chip layout. Blue represents Al traces, gold AuCu traces. Pads near upper edge of chip provide two independent flux lines; Al wirebonded jumpers couple left and right halves of each of the two flux lines. Pads near lower edge of chip are used to supply current pulses to the read-out SQUID and to sense any resulting voltage. Chip is 2 mm on a side. (b) Photograph of completed device. Segments of flux lines are visible to left and right of SQUID, which surrounds the two qubits.

Figure 3 shows the layout of our device. The read-out SQUID has a calculated inductance L_s = 358 pH, and each of the two qubits it encloses has a calculated inductance L_Q = 143 pH. The calculated mutual inductance between each qubit and the SQUID is 61 pH. One pair of series-connected flux bias lines is arranged near the top of the SQUID and a second near the bottom; thus, flux in qubit 1 (2) is supplied predominantly by the upper (lower) flux lines. The mutual inductance between each qubit and its associated flux lines was designed to be 4-5 pH, enabling us to apply $\sim 2\Phi_0$ with a current of 1 mA. This criterion dictated the relatively large qubit inductances compared with those in previous experiments [3, 4]. The wiring to the SQUID that provides current pulses and senses any resulting voltage was laid out symmetrically to minimize spurious inductive coupling to the SQUID and qubits.

We fabricated the device on an oxidized Si substrate using electron-beam lithography and double-angle evaporation to form the Al-AlOx-Al tunnel junctions. The Al lines for the qubit and SQUID loops are 1 μm wide, and for the flux bias 10 μm wide. Each SQUID junction was 175 x 200 nm^2 with a capacitance of 6.5 fF, estimated with a specific capacitance of 100 fF/μm^2 and a stray capacitance of 3 fF, obtained by separate experiments on SQUIDs with a range of areas. The junction critical current was 0.44 μA. For qubits 1 and 2, the larger junctions had areas of 250 x 250 nm^2 and 180 x 200 nm^2, critical currents I_0 (scaled from SQUID junctions) of 0.79 μA and 0.46 μA, and α-values of 0.49 and 0.68, respectively. The different junction parameters were chosen to increase the probability of obtaining one viable qubit; in fact, qubit 2 displayed good characteristics. A AuCu film deposited and patterned prior to the Al deposition provided quasiparticle traps near the junctions, shunts on each of the four flux lines, and series resistors on each end of the pulse line and sense lines.

III. Quantum Coherence in a Flux Qubit

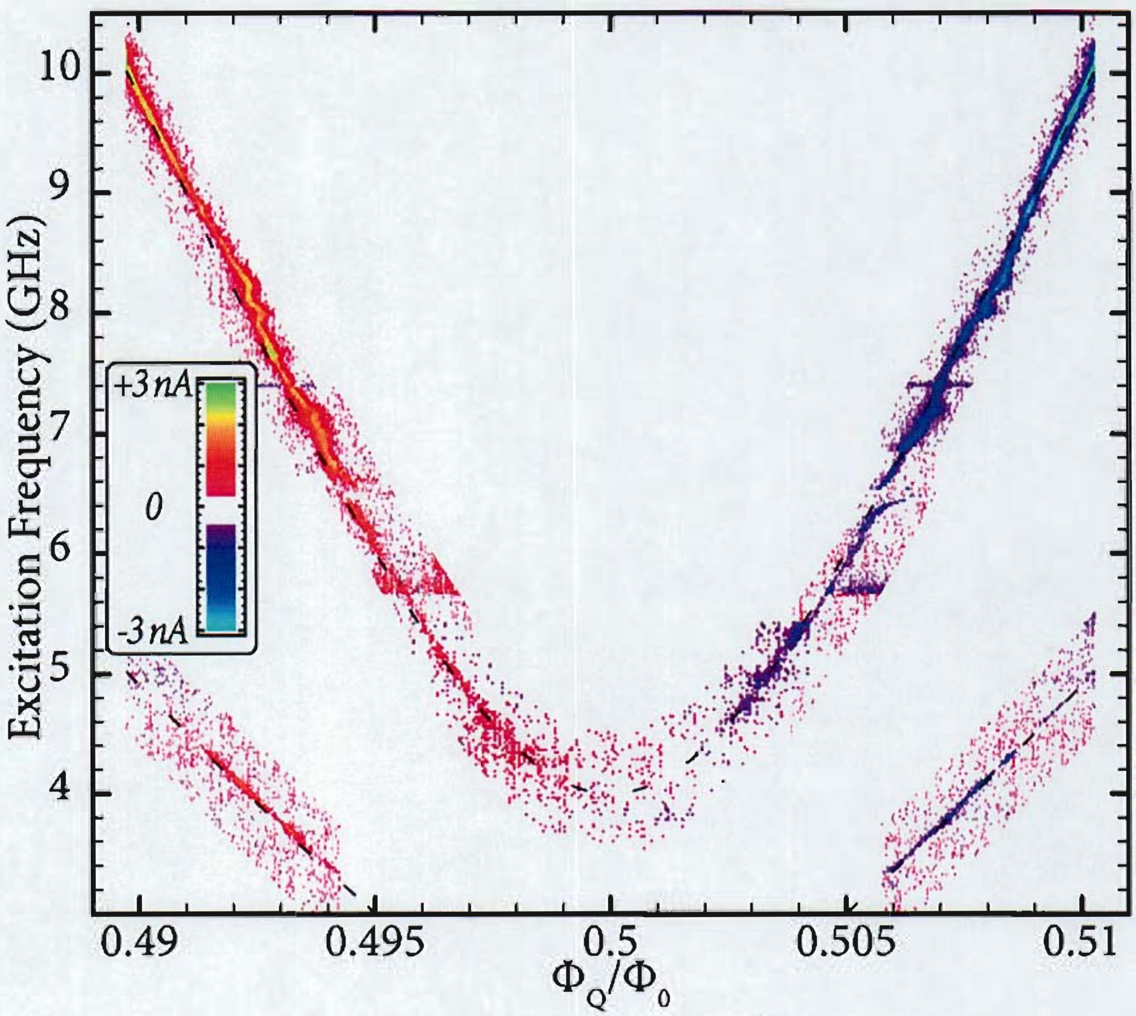

Fig. 4. Spectroscopy of flux qubit.

We have observed quantum coherence in qubit 2 [5]. Figure 4 shows the excitation frequency versus the qubit flux obtained in a computer-controlled experiment in which the microwave frequency and qubit flux are varied with a constant flux in the readout SQUID. Spectroscopic peaks are on the right and dips on the left; there is a well-defined splitting of $\Delta/h = 3.99$ GHz at the degeneracy point. The expected cavity resonance is clearly visible at about 6 GHz. From this spectrum, we deduce a flux-to frequency conversion of 896 MHz/mΦ_0. The outer two branches correspond to two-photon transitions, fitted with the same parameters as the single-photon spectrum.

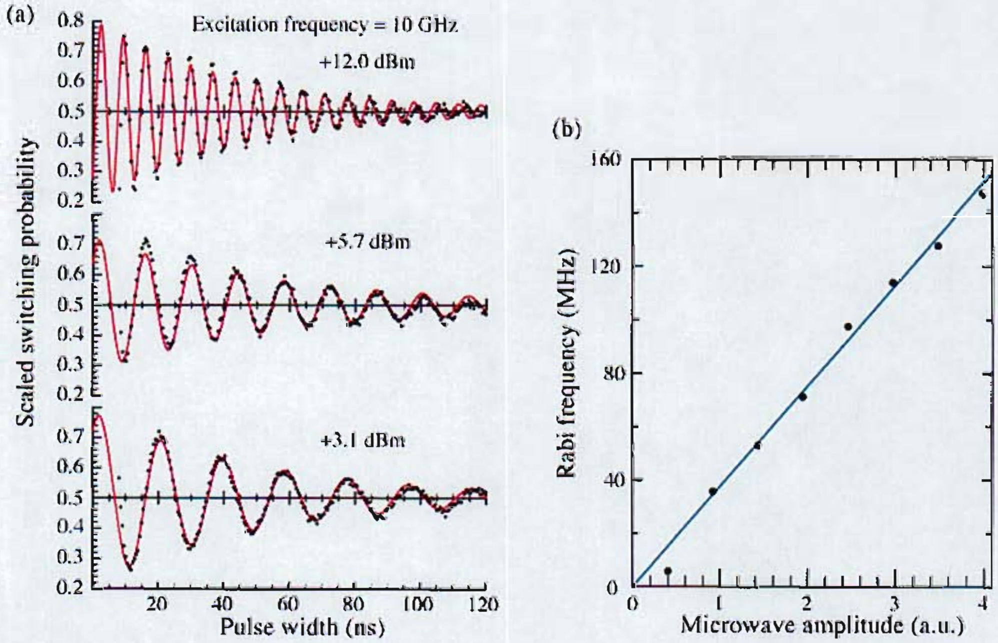

Fig. 5. (a) Rabi oscillations of flux qubit for three different microwave powers. (b) Rabi frequency vs. microwave drive amplitude.

Figure 5(a) shows a series of Rabi oscillations obtained by applying a pulse of microwaves to the qubit just before measuring its flux state. The switching probability, scaled to the fidelity of the readout SQUID, is plotted versus the duration of the microwave pulse. Fits of exponential decaying sine waves to the data reveal relatively large contrasts – as high as 63% – and Rabi decay times as high as 78 ns. Figure 5(b) shows that the measure Rabi frequency scales linearly with the microwave amplitude, as predicted.

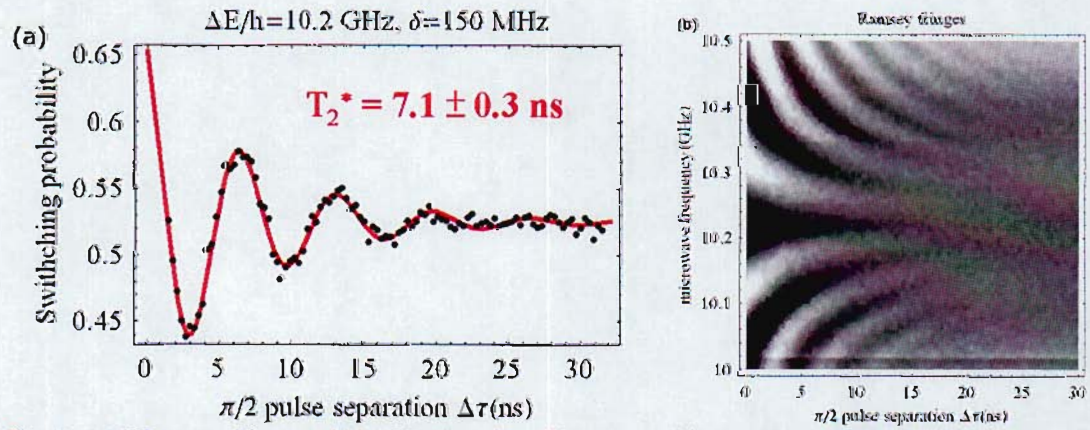

Fig. 6. (a) Ramsey fringe at 150 MHz detuning. (b) Ramsey fringe measurement containing 80 excitation frequencies.

Figure 6 illustrates Ramsey fringes, in which two $\pi/2$ microwave pulses are applied sequentially to the qubit. Figure 6(a) plots the SQUID switching probability versus the time interval between the two pulses for a microwave frequency f_m that is slightly off-resonance. A fit to these oscillations yields a decoherence time T_2* of 7.1 ± 0.3 ns. The Ramsey fringe frequency is expected to be proportional to $|f_m - f_q|$, where f_q is the resonant frequency of the qubit. This behavior is clearly demonstrated in Fig. 6(b), which yields $f_q = 10.22$GHz.

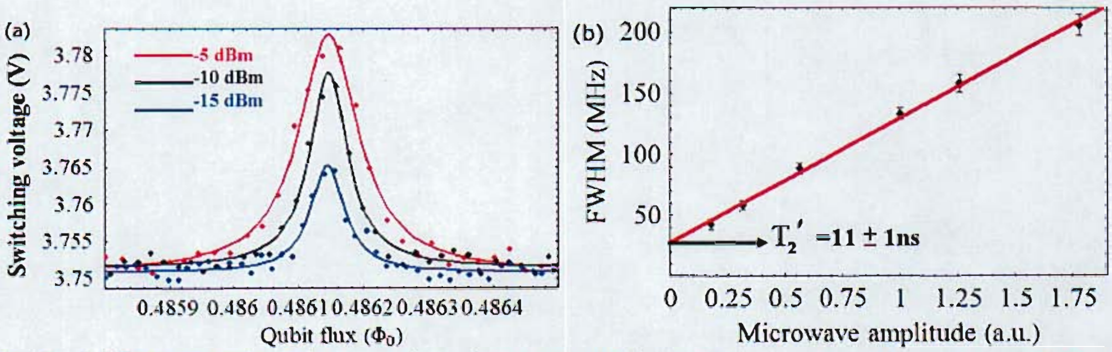

Fig. 7 (a) Spectroscopic peaks at varying microwave amplitude. Excitation frequency was 10.2 GHz. (b) Peak linewidth as a function of microwave amplitude.

Another measure of decoherence may be obtained from the dependence of spectroscopic linewidth on microwave amplitude. In the limit of strong driving, this dependence is approximately linear and extrapolates at zero driving amplitude to a linewidth corresponding to the inhomogeneous dephasing time T_2'. Figure 7 shows linewidth measurements at a qubit resonant frequency of 10.2 GHz, and the extrapolation of $T_2'=11.1 \pm 1$ ns from this data.

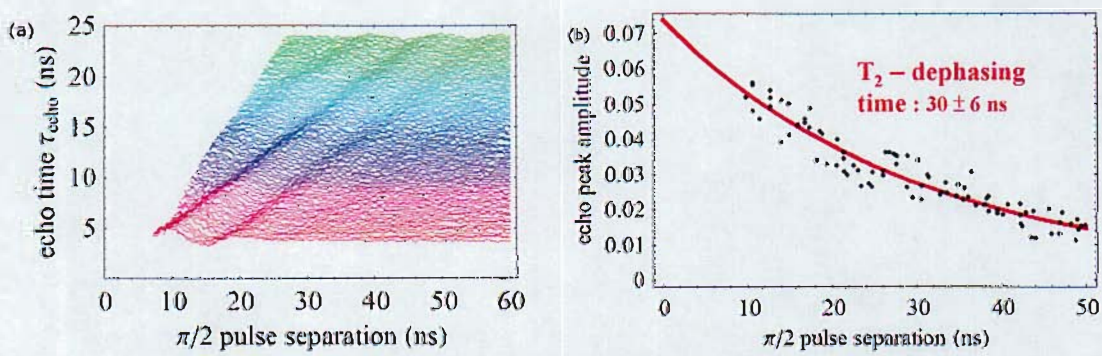

Fig. 8 (a) Echo-corrected Ramsey fringes. (b) Decay of echo envelope.

We performed echo-corrected Ramsey fringe measurements in which a π microwave pulse was inserted between the two $\pi/2$ pulses. Data for a range of π pulse positions is shown in Fig. 8(a). The echo pulse corrects for inhomogeneous dephasing, so that the peak of the echo envelope decays with the homogeneous dephasing time T_2. In Fig. 8(b) we obtain a value $T_2 = 30 \pm 6$ ns. The overall dephasing rate is expected to be the sum of the homogeneous and inhomogeneous contributions, that is, $(T_2^*)^{-1} = (T_2)^{-1} + (T_2')^{-1}$. We find $[(T_2)^{-1} + (T_2')^{-1}]^{-1} = 8.1 \pm 1.7$ ns, which is consistent with the measured value $T_2^* = 7.1 \pm 0.3$ ns.

IV. Effect of Hot Quasiparticles in the Readout SQUID on the Relaxation Time of a Flux Qubit

The flux states are read out with a dc SQUID inductively coupled to the qubits. This device offers high flux sensitivity readout due to the highly nonlinear dynamic conductance of the SQUID when operated at a bias point near its critical current. However the switching of the SQUID to the voltage state also results in the breaking of Cooper pairs, which compromises the low-noise, non-dissipative quality that makes superconducting devices promising candidates for quantum computing.

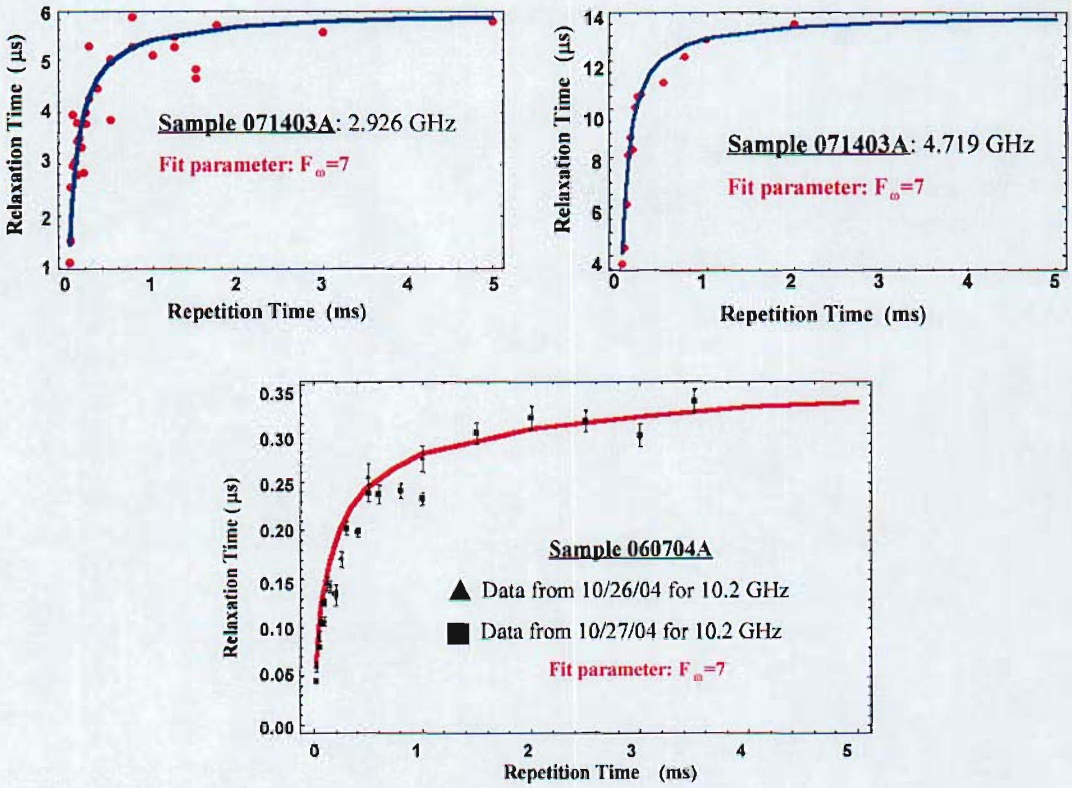

Fig.9 Qubit relaxation time as a function of repetition time for two samples. Fits from the model (solid red and blue curves) are shown overlaying the data points. The open fit parameters for each plot are given.

The number density of these nonequilibrium quasiparticles, and hence the equivalent Nyquist noise spectrum, is roughly proportional to the SQUID critical current and the length of time the SQUID remains at the 2Δ-gap. The quasiparticles are removed through pair-recombination, a process that takes place on a time scale dependent on their effective temperature. Recombination lifetimes in Al at thermal equilibrium with the bath can be extremely large compared with nanosecond timescales required of a qubit. For pulsed readout, the effect of the long recombination time should be directly observable by setting a limit on the repetition rate of the current pulses in the SQUID. Below this limit, the rate of quasiparticle generation exceeds the rate of quasiparticle removal in the SQUID, and qubit decoherence times may be drastically reduced by the resultant increase in dissipative noise currents in the SQUID, which appear as flux noise in the qubits. Indeed, we have observed [Fig. 9] this effect in relaxation time measurements of two separate samples. We see the upper limit to the repetition rate in the relaxation time measurements for both samples to be around 1 kHz. A viable qubit readout device will require a much greater repetition rate.

To understand this effect and to explore the possibility of mitigating the limitations it imposes, we have developed a model for the quasiparticle generation and recombination in our SQUID. We take into account two effects of the high-energy recombination phonons in the aluminum film of the SQUID: the pair-breaking process and phonon-trapping. We assume the quasiparticle recombination rate per unit density, R, and the pair-breaking lifetime of the 2Δ-phonons, τ_B, are constants and use typical theoretical values. We also assume that the gap anisotropy smearing, g, is constant at $0.05\Delta_{Al}$. The phonon-trapping factor, F_ω, is the average number of pairs a given phonon will break before escaping to the substrate. We leave F_ω as a free parameter. The measured background relaxation time of the qubits is Γ_0, which is independent of the repetition rate, τ_{rep}^{-1}.

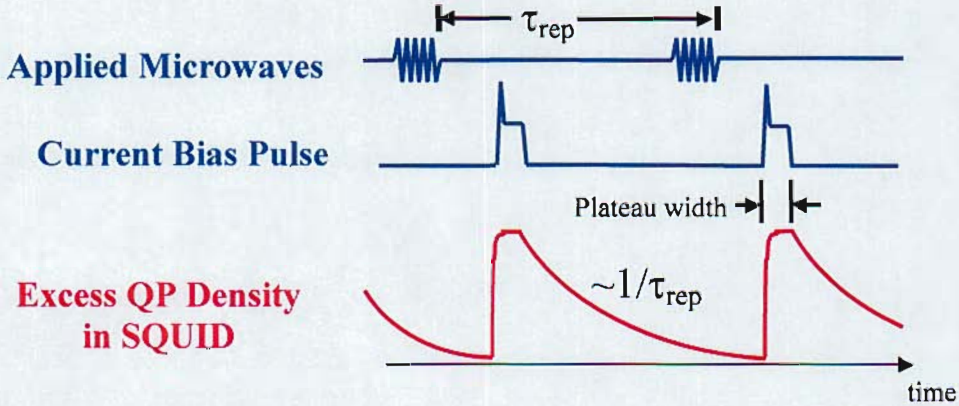

Fig. 10 Microwave and SQUID current pulse sequence, showing the resultant nonequilibrium quasiparticle density in the read-out SQUID. The qubit samples the noisy "hot" quasiparticle environment just before each subsequent microwave pulse.

For every point in a train of pulse sequences [Fig. 10] in the SQUID and qubit system, we solve the coupled Rothwarf-Taylor equations, which describe the quasiparticle and 2Δ-phonon densities in the SQUID. The effect of the phonons is largely to retard the effective recombination rate of the quasiparticles.

The quasiparticle density solution has three regimes of interest: the driving regime, when the SQUID is switched and generation rate exceeds the recombination rate; the saturation regime, when the recombination rate balances the generation rate; and the decaying regime, when the SQUID is restored to the zero-voltage state and the quasiparticle densities decrease hyperbolically with time.

The qubit is turned on with a microwave pulse after the SQUID has been in the decaying regime for a time $\sim\tau_{rep}$. The quasiparticle number density is calculated at this time, and converted to an effective temperature, T*, by the usual BCS relation. We then calculate the equivalent quasiparticle noise current spectrum in the SQUID at temperature T* and subsequently the flux noise it induces on the qubits. From the standard spin-boson treatment, we arrive at a qubit relaxation time from this quasiparticle number density. By repeating the calculations for many repetition times in the range of 25–5000 ns, we obtain the solid curves shown in Fig. 9.

By solving the coupled 2Δ-phonon and quasiparticle rate equations and using the measured parameters and one fit parameter (F_{ω}) we obtain a reliable fit for the relaxation time dependence on the current pulse repetition rate for the two samples at two different frequencies. It is particularly gratifying that the best fit for two different samples is obtained for the same value of F_{ω}. From this analysis, we conclude that efficient phonon-substrate coupling—particularly around the SQUID junctions—will greatly increase the effective quasiparticle recombination rates. Additionally, since the quasiparticles are generated in the junctions the presence of normal-metal traps, each with a high-quality NS interface, near the SQUID junctions should drastically reduce the diffusion of large quasiparticle densities around the SQUID loop and thus minimize the resultant flux noise in the qubits. Alternatively, one should adopt an inductive readout scheme in which the SQUID remains in the zero voltage regime.

V. Entangling Flux Qubits with a Bipolar Dynamic Inductance

To implement a quantum algorithm, one must be able to entangle multiple qubits, so that an interaction term is required in the Hamiltonian describing any two qubit system [6]. For two superconducting flux qubits, the natural interaction is between their magnetic fluxes. Thus, for two flux qubits arranged so that a flux change in one qubit can alter the flux of the second qubit, the coupled-qubit Hamiltonian takes the form

$$H = H_1 + H_2 - (K/2)\sigma_z^{(1)}\sigma_z^{(2)}. \qquad (1)$$

Here, H_1 and H_2 are the Hamiltonians of the separated qubits 1 and 2, and $\sigma_z^{(1)}$ and $\sigma_z^{(2)}$ are the Pauli spin-1/2 operators for qubits 1 and 2. The parameter K characterizes the coupling strength; for $K < 0$, the minimum energy configuration for this system is with the qubits antiparallel. For two qubits coupled through a mutual inductance M_{qq}, the interaction strength K_0 is given by

$$K_0 = -2M_{qq}\, |I_q^{(1)}||I_q^{(2)}|, \tag{2}$$

and will always be present in any practical layout [7]; $I_q^{(1)}$ and $I_q^{(2)}$ are the supercurrents in qubits 1 and 2.

Pulse sequences for generating entanglement have been derived for several superconducting qubits with fixed interaction energies [8], [9]. However, entangling operations can be much more efficient if the interaction can be varied and ideally turned off during parts of the manipulation. Although switchable couplings have been proposed for flux qubits [10], [11], these approaches require the rapid switching of fluxes on the order of a flux quantum Φ_0 which is difficult to implement. We have devised a coupling scheme for flux qubits whereby the interaction is adjusted by changing a relatively small current which can be varied rapidly with existing pulse technology. For suitable device parameters, the sign of the coupling can also be changed, thus making it possible to null out the direct interaction between the flux qubits. Furthermore, the same device can be used to vary the coupling and to read out the flux states of the qubits. A variable coupling scheme for charge-based superconducting qubits has been suggested recently [12], but, to our knowledge, no feasible variable coupling has previously been proposed to exploit the advantages of flux qubits.

The coupling mechanism for our scheme [Fig. 11(a)] is the circulating current J in a dc Superconducting QUantum Interference Device (SQUID), in the zero voltage state, which is coupled to each of the two identical qubits through an identical mutual inductance M_{qs}. A variation in the flux applied to the SQUID, Φ_s, caused by one of the qubits switching between its two flux states, changes J as determined by $L_D^{-1} = \partial J/\partial\Phi_s$, the inverse dynamic inductance. This change in J alters the flux coupled from the SQUID to the second qubit, leading to an interaction energy between the two qubits, K_s, which is proportional to L_D^{-1}. The coupling strength K_s takes the form

$$K_s = -2M_{qs}^2\, |I_q^{(1)}||I_q^{(2)}|\, \mathrm{Re}(\partial J/\partial\Phi_s). \tag{3}$$

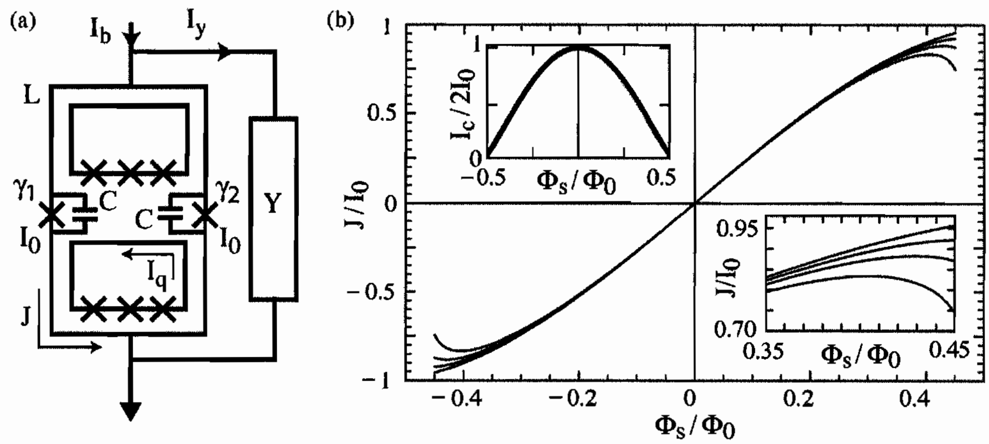

Fig. 11. (a) Layout of SQUID-based coupling scheme. Element Y represents the admittance of the SQUID bias and measurement circuitry. (b) Response of SQUID circulating current J to applied flux Φ_s for $I_b/I_c(0.45\ \Phi_0) = 0, 0.4, 0.6, 0.85$ and $\beta_L = 0.092$. Inset in lower right shows variation of J with I_b near $\Phi_s = 0.45\Phi_0$ and upper left inset shows modulation of I_c with Φ_s.

For reasonable device parameters, the sum of K_s and the direct mutual interaction between the qubits, K_0, can be as large as -0.3 GHz. For a particular range of values of the screening parameter $\beta_L = 2LI_0/\Phi_0$ and for fixed magnetic flux, L_D^{-1} can be reduced to zero and even made negative by changing the bias current I_b [Fig. 11(b)]; here $I_b < I_c(\Phi_s)$, the critical current for which the SQUID switches out of the zero voltage state at zero temperature in the absence of quantum tunneling. The ability to change the sign of L_D^{-1} makes it possible to null out K_0, yielding a vanishing net interaction so that the qubits are truly isolated [Fig. 12]. In previous single qubit experiments [4], including our own measurements, the qubit state is determined by coupling the qubit screening flux to a similar dc SQUID to which rapid pulses of I_b are applied to measure $I_c(\Phi_s, T)$. Thus, the existing measurement technology allows for I_b to be varied on this same timescale of a few nanoseconds, so that a single dc SQUID can be used to measure the flux state of two qubits and to couple them together controllably.

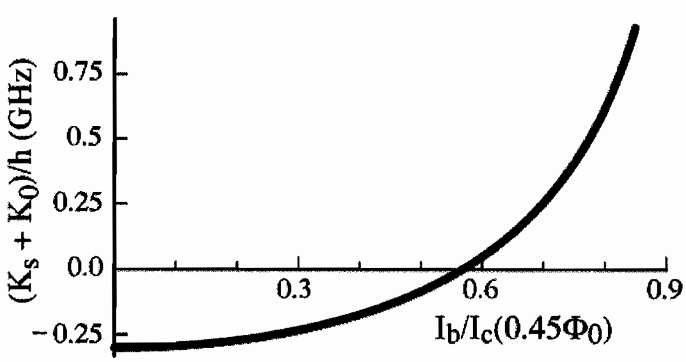

Fig. 12. Variation of K with I_b for $\Phi_s = 0.45\ \Phi_0$ and device parameters given in text.

When combined with Rabi pulses to generate single qubit rotations, our coupling scheme can perform entangling operations on the two flux qubits. Our calculations of the coupler dynamics show that the quantum Controlled-NOT (CNOT) logic gate between two flux qubits can be achieved with the pulse sequence shown in Fig. 13. After the qubits are manipulated individually with tuned microwave pulses, $\varepsilon_1(t)$ and $\varepsilon_2(t)$, the coupling strength K is pulsed on for about 10 ns, and a final set of microwave pulses is applied. The total duration for this operation is about 30 ns. Our analysis of the dissipation in the bias circuitry indicates that the decoherence due to the coupler, as characterized by the Leggett dissipation parameter α, can be reduced to about 10^{-4} for a reasonable choice of series resistance on the bias current leads, 2.4 kΩ. This value of α corresponds to a decoherence time of 500 ns, which is comparable with times currently achieved experimentally at the degeneracy point, but significantly longer than those observed away from the degeneracy point.

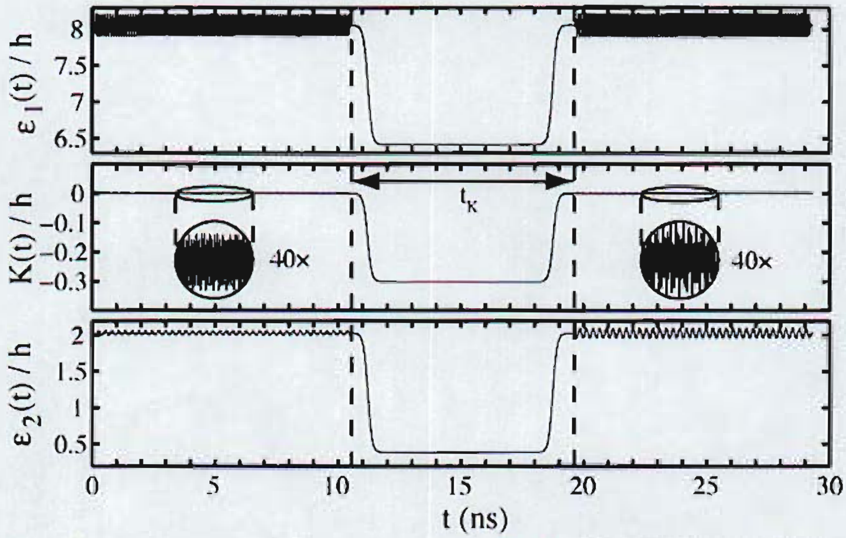

Fig. 13. Pulse sequence for producing CNOT gate. Bias current pulsed to turn on interaction in central region, while pulses of microwave flux drive the qubit biases, $\varepsilon_1(t)$, $\varepsilon_2(t)$, for producing single qubit rotations.

Finally, we note that this approach to entangling flux qubits should be readily scalable, for example, with the layout of Fig. 14. With the application of current pulses of appropriate magnitudes, each SQUID can be used to entangle and readout two qubits.

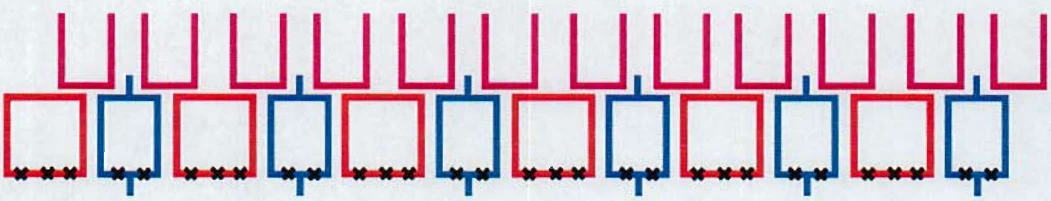

Fig. 14. Chain of flux qubits with dc SQUIDs arranged to provide variable nearest neighbor coupling along with readout of qubits.

VI. Concluding Remarks

During the course of the project, we have developed a fabrication process for flux qubits and assembled the necessary infrastructure to characterize them. We have made detailed studies of the decoherence times obtained from Ramsey fringes, spectroscopic linewidth, and spin echoes and shown that they are self-consistent. We have made careful measurements of the effects of nonequilibrium quasiparticles generated in the readout SQUID, and developed a theory that is in excellent agreement with the data. From these results, we conclude that it is imperative to develop alternative readout schemes that do not require the SQUID to switch to the voltage state, for example, by measuring the change in the inductance of the SQUID with enclosed magnetic flux. We have completed a theory for a novel technique to entangle qubits using the readout SQUID as an inductive entangling device. We hope to implement this scheme in the near future.

We did not succeed in our stated goal of entangling two qubits experimentally. This failure was due entirely to the virtual demise of the electron-beam writing system in the Microfabrication Facility at UC Berkeley over the first half of 2005. The system has degenerated to the point where it is almost impossible to achieve consistent results from run to run. Despite the great difficulties in writing devices with the appropriate parameters, after some 8 months of endeavor, we succeeded in producing a chip with two qubits that is currently under investigation.

Three more papers are currently being written for submission to journals by the end of 2005: (a) A paper on the theory of the three-junction flux qubit in the limit where the loop inductance is non-negligible; (b) a paper describing in detail our experiments on quantum coherence in the flux qubit; (c) a paper describing our experiments on the decoherence in the flux qubit induced by nonequilibrium quasiparticles, along with the theory of these effects.

VII. References

[1] J. Clarke *et al.*, *Science* **239**, 992-997 (1988).
[2] S. Linzen *et al.*, *Rev. Sci. Instrum.* **75**, 2541 (2004).
[3] J. Mooij *et al.*, *Science* **285**, 1036 (1999).
[4] I. Chiorescu *et al.*, *Science* **299**, 1869 (2003).
[5] B.L.T. Plourde *et al.*, *Phys. Rev. B* **72**, 060506 (2005).
[6] B.L.T. Plourde *et al.*, *Phys. Rev. B* **70**, 140501 (2004).
[7] J. Majer *et al.*, *Phys. Rev. Lett* **94**, 090501 (2005).
[8] T. Yamamoto *et al.*, *Nature* **425**, 941 (2003).
[9] F. Strauch *et al.*, *Phys. Rev. Lett.* **91**, 167005 (2003).
[10] J. Mooij *et al.*, *Science* **285**, 1036 (1999).
[11] J. Clarke *et al.*, *Physica Scripta* **T102**, 173 (2002).
[12] D. Averin and C. Bruder, *Phys. Rev. Lett.* **91**, 057003 (2003).